Improvement of Modal Matching Image Objects in Dynamic Pedobarography using Optimization Techniques

Luísa Ferreira Bastos[1], João Manuel R. S. Tavares[2]

[1, 2]Laboratório de Óptica e Mecânica Experimental
do Instituto de Engenharia Mecânica e Gestão Industrial,
[2]Departamento de Engenharia Mecânica e Gestão Industrial,
Rua Dr. Roberto Frias, s/n, 4200-465, Porto, PORTUGAL
lbastos@fe.up.pt, tavares@fe.up.pt

Abstract. The paper presents an approach for matching objects in dynamic pedobarography image sequences, based on finite element modeling and modal analysis. The determination of correspondences between objects' nodes is here improved using optimization techniques and, because the elements number of each object is not necessarily the same, a new algorithm to match excess nodes is proposed. This new matching algorithm uses a neighborhood criterion and can overcome some disadvantages that the usual matching "one to one" in various applications can have. The proposed approach allows the determination of correspondences between 2D or 3D objects and will be here considered in dynamic pedobarography images.

1 Introduction

One problem of several areas of computational vision is the determination of objects correspondences in different images and on the computation of robust canonical descriptors used for the recognition of 2D or 3D objects, either rigid or non-rigid.

In this paper, a methodology to address the above problem is presented, based in the approach initially proposed by Sclaroff [1], [2], improved by us through the use of optimization algorithms in the matching search step, and a new method to determine matches between nodes that could not be considered in this optimization phase (see section 4). With this new method, we can successfully match objects with different number of points and also overcome some disadvantages that the usual match "one to one" can present in various real applications, because with that algorithm we can now have matches of type "one to many" and vice-versa.

Application results of the proposed matching methodology improved, and of the new "one to many" and vice-versa matching algorithm, to the analysis of objects represented in dynamic pedobarography image sequences are discussed.

1.1 Background

There is an eigen methods class [1], [2], that derives its parameterization directly from the data shape. Some of these techniques also try to determine, explicitly and automatically, the correspondences between characteristic points' sets, while others avoid specifying correspondences based in characteristics, but try to match images using more global approaches. Each eigen method decomposes the object deformation in an orthogonal and ordered base.

Usually, the matching problem resolution methods include restrictions that prevent inadequate matches according to the considered criteria. Examples of these restrictions are: the order [3], [4]; rigidity restriction [3], [4]; unicity [5]; visibility [6]; and proximity [2]. To determine the correspondences it is used, for example, the correlation between images (i.e., images similarity is assumed) [7]; points proximity [8]; or disparity fields smoothness [3]. The matching problem can be interpreted as an optimization problem, where the objective function can depend, for example, on any relation mentioned above and the restrictions must form a non-empty space of possible solutions for the optimization problem. To solve the optimization problem it can be used dynamic programming [3], graphs [4] and convex minimization [7]. Non-optimal approaches include, for example greedy algorithms [9], simulated annealing [10], relaxation [5], etc.

Belongie [11] applied an optimization technique, similar to the one used in this work, to determine the correspondences between two objects using shape contexts. Although shape description algorithms have usually a higher computational efficiency, the modeling methodology presented here has the major advantage of attributing a physical behavior to each object to be modeled through the consideration of a virtual material.

2 Dynamic Pedobarography

Pedobarography refers to measuring and visualizing the distribution of pressure under the foot sole. The recording of pedobarographic data along the duration of a step in normal walking conditions permits the dynamic analysis of the foot behavior; the introduction of the time dimension augments the potential of this type of clinical examination as an auxiliary tool for diagnostics and therapy planning [12], [13].

The basic pedobarography system consists of glass or acrylic plate transilluminated through its polished borders in such a way that the light is internally reflected; the plate is covered on its top by a single or dual thin layer of soft porous plastic material where the pressure is applied (see Fig. 1) [13].

Using a practical set-up as the one shown in Fig. 2, a time sequence of pressure images is captured; Fig. 3 shows two of the images captured in a sample sequence (displayed with inverted brightness); the image data is very dense, as opposed to other used measuring methods, and very rich in terms of the information it conveys on the interaction between the foot sole and the flat plate [13].

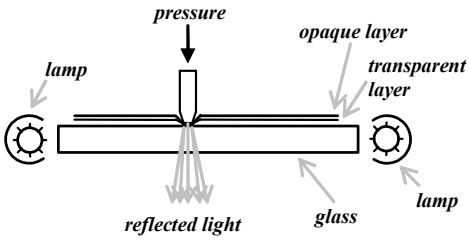

Fig. 1. Basic (pedo)barography principle [13]

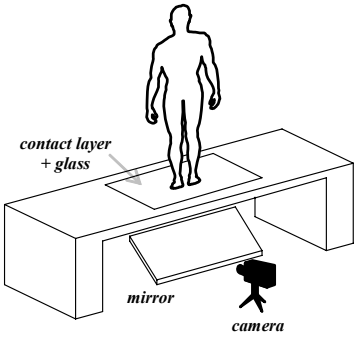

Fig. 2. Set-up of a basic pedobarography system [13]

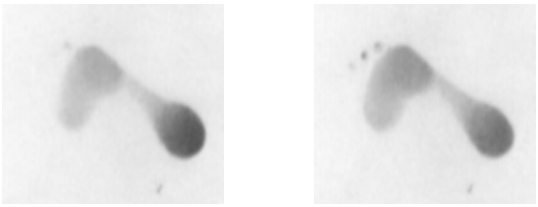

Fig. 3. Two consecutive images of a sample pedobarography images sequence

3 Objects Model

In the initial stages of this work [2], [13], the object contours in each image were extracted and the matching process was oriented to the contours pixels. However, an additional problem is present: the possibility that along the images sequence various contours will merge or split. In order to accommodate this possibility a new model was developed [13], similar to the one used in various applications with controlled environment, such as in face analysis and recognition [14], [15]. The brightness level of each pixel is considered as the third co-ordinate of a 3D surface point. The resulting single surface model solves the two aforementioned problems [13].

The use of the surface model also simplifies the consideration of isobaric contours, which are important in pedobarographic analysis, either for matching contours of equal pressure along the time sequence or for matching contours of different pressure in a single image [13].

The following sections describe the object models used and their construction. Each model has its own advantages and shortcomings; for every particular problem, the best choice must be made [13].

3.1 Contour Model

Two modeling approaches were used to determine the correspondence between two contours in distinct images:

- A single 2D isoparametric Sclaroff model is used for each contour. In building this type of element, no previous ordering of the nodes is required; Gaussian shape functions are used. The method to determine the mass and stiffness matrices for this 2D element is described, for example, in [1], [2].
- Each contour is built by linear axial 2D finite elements. For this type of discretization a previous ordering of the contour nodes is required. The matrix formulation for these elements can be found in [2], [16], for example.

Standard image processing and analysis techniques are used to determine the contour pixels [2], namely thresholding, edge enhancement, hysteresis line detection and tracking. For example, Fig 4(b) and Fig. 4(c) show an intermediate result and the final contour determination for the image in Fig. 4(a).

3.2 Surface Model

For the surface model, two approaches were also used [2], [13]:

- A single 3D isoparametric Sclaroff finite element model is used for each surface. Again, it must be noticed that there is no requirement for previous ordering of the nodes. The matrix building for these finite elements can be found in [1], [2].
- Each surface is built by linear axial 3D finite elements (Fig. 5). The previous ordering of the surface nodes is required. The matrix formulation for these finite elements can be found in [2], [16], for example.

The method to determine the nodes that form the surface in each image can be summarized as follows [2], [13]:

1. Noise pixels (i.e., pixels with brightness lower than a calibration threshold) are removed and a Gaussian-shaped smoothing filter is applied to the image (Fig. 6(a));
2. The circumscribing rectangle of the object to be modeled is determined and the image is sampled within that area (Fig. 6(b));
3. A 2D Delaunay triangulation is performed on the sampled points, using the point brightness as the third co-ordinate;
4. The triangular mesh is simplified using a decimation algorithm in order to reduce the number of nodes and thus the computational cost;
5. A Laplacian smoothing algorithm is used to reduce the high frequency noise associated to the mesh;

6. A scale change is performed on the third co-ordinate (derived from brightness) in order to have similar ranges of values in all co-ordinates (Fig. 6(c)).

(a) (b) (c)

Fig. 4. (a) Image (negated) where contours must be found; (b) Result image after edge enhancement; (c) Contours obtained by a line detection and tracking algorithm with hysteresis

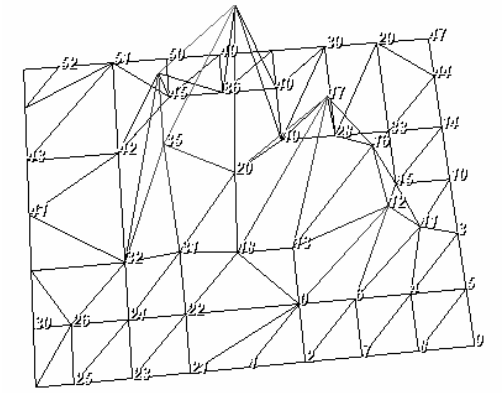

Fig. 5. Modeling of a surface by a set of axial 3D finite elements (each node is connected to its neighbors through axial elements)

(a) (b) (c)

Fig. 6. (a) Image (negated) after noise removal and Gaussian filtering; (b) Object sampling; (c) Resulting surface

3.3 Isobaric Contour Model

As in the two previous models, the approaches used to match isobaric contours and to determine the deformation energy are [2], [13]:

- A single Sclaroff isoparametric finite element, either 2D or 3D, to model each contour.
- Linear axial finite elements, either 2D or 3D, to build the contours.

The isobaric contours are extracted (Fig. 7) after using the procedure described in the previous section.

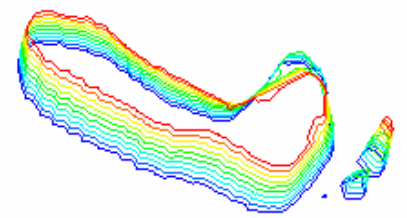

Fig. 7. Ten isobaric contours extracted from the surface in Fig. 6(c)

4 Matching Methodology

Fig. 8 displays a diagram of the adopted matching methodology. The locations of the image data points $X = [X_1 \ldots X_m]$ in each image are used as the nodes for building a finite element model of elastic material. Next, the eigenmodes $\{\phi\}_i$ of the model are computed, providing an orthogonal description of the object and its natural deformations, ordered by frequency. Using a matrix based notation, the eigenvectors matrix $[\Phi]$ and the eigenvalues diagonal matrix $[\Omega]$ can be written as in eq. (1) for 2D objects and as in eq. (2) for 3D objects. The eigenvectors, also called shape vectors, for each mode [1], [2], [16], [17], describe how each mode deforms the object by changing the original data point locations: $X_{deformed} = X + a\{\phi\}_i$.

The first three (in 2D) or six (in 3D) modes are the rigid body modes of translation and rotation; the remaining modes are non-rigid [1], [2], [16], [17]. In general, lower frequency modes describe global deformations while higher frequency modes essentially describe local deformations. This type of ordering from global to local behaviour is quite useful for object matching and comparison.

The eigenmodes also form an orthogonal, object-centred co-ordinate system for the location of the point data, i.e., the location of each point is uniquely described, in

terms of each eigenmode displacement. The transformation between the Cartesian image co-ordinates and the modal system co-ordinates is achieved through the eigenvectors of the finite element model.

Two sets of image data points, corresponding to two different images in a sequence, are to be compared in the modal eigenspace. The main idea is that the low order modes of two similar objects will be very close even in the presence of an affine transformation, a non-rigid deformation, a local shape variation, or noise [1], [2].

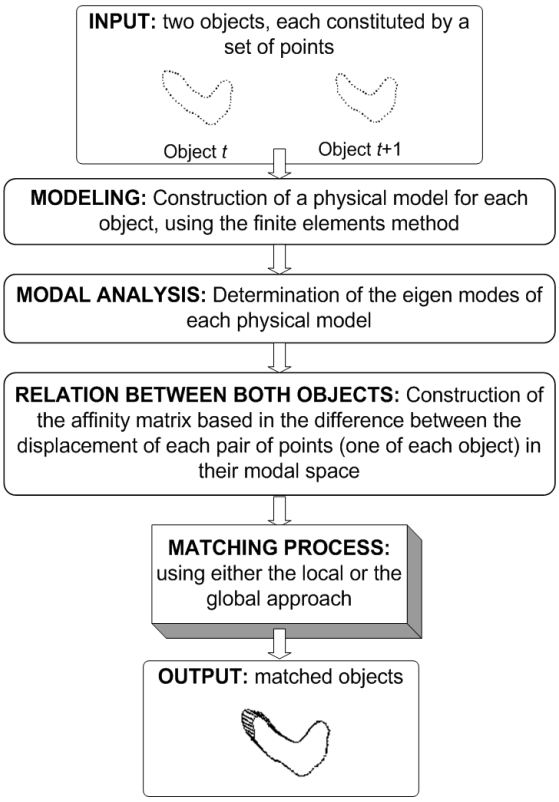

Fig. 8. Diagram of the adopted methodology

$$\left[\Phi\right]=\left[\left\{\phi\right\}_1\middle|\cdots\middle|\left\{\phi\right\}_{2m}\right]=\begin{bmatrix}\left\{u\right\}_1^T\\ \vdots\\ \left\{u\right\}_m^T\\ \left\{v\right\}_1^T\\ \vdots\\ \left\{v\right\}_m^T\end{bmatrix} \text{ and } \left[\Omega\right]=\begin{bmatrix}\omega_1^2 & & 0\\ & \ddots & \\ 0 & & \omega_{2m}^2\end{bmatrix}, \tag{1}$$

$$[\Phi]=\left[\{\phi\}_1\middle|\cdots\middle|\{\phi\}_{3m}\right]=\begin{bmatrix}\{u\}_1^T\\ \vdots\\ \{u\}_m^T\\ \{v\}_1^T\\ \vdots\\ \{v\}_m^T\\ \{w\}_1^T\\ \vdots\\ \{w\}_m^T\end{bmatrix} \text{ and } [\Omega]=\begin{bmatrix}\omega_1^2 & & 0\\ & \ddots & \\ 0 & & \omega_{3m}^2\end{bmatrix}. \quad (2)$$

Using the above concept, data correspondence is obtained by modal matching. Two matching search methods are considered: (1) a local search or (2) a global search. Both methods use an affinity matrix [Z], constructed from the Euclidian distance between the characteristic vectors of each model, whose elements are, for 2D and for 3D, respectively:

$$Z_{ij}=\left\|\{u\}_{t,i}-\{u\}_{t+1,j}\right\|^2+\left\|\{v\}_{t,i}-\{v\}_{t+1,j}\right\|^2, \quad (3)$$

$$Z_{ij}=\left\|\{u\}_{t,i}-\{u\}_{t+1,j}\right\|^2+\left\|\{v\}_{t,i}-\{v\}_{t+1,j}\right\|^2+\left\|\{w\}_{t,i}-\{w\}_{t+1,j}\right\|^2. \quad (4)$$

The local search was previously implemented [1], [2], [13] and basically it consists in seeking each row of the affinity matrix for its lowest value, considering the associated correspondence if that value is also the lowest of the associated column. This method has the main disadvantage of disregarding the object structure as it searches for the best match for each node.

The global search, proposed in this work, consists in describing the matching problem as an assignment problem [18], [19], and solving this last using an appropriate algorithm [20], [21], [22].

Case the number of nodes of both objects is not the same, with the usual matching restriction of type “one to one”, there will be, necessarily, nodes that will not be matched. The solution found [20] was initially to add fictitious nodes to the model with fewer points, solving the requirement of the matrix involved in the optimization process (assignment problem) having, necessarily, to be square. All fictitious nodes have a zero matching cost associated. After the global search, the excess nodes (real nodes matched with fictitious points) are matched adequately (with real nodes), using a neighborhood criterion. In this way matches of type “one to many” or vice versa are allowed for the “extra” nodes. We will call this method *ADCom*.

5 Results

The methodology just presented was integrated in a generic software platform for deformable objects matching [23], previous developed using Microsoft Visual C^{++}, the Newmat [24] library for matrix computation and the VTK - The Visualization Toolkit [25], [26] for 3D visualization, mesh triangulation, simplification and smoothing, and for isobaric contours extraction.

This section presents some obtained results with dynamic pedobarography images, using the methodology previously described.

The first example presents the matching of two contours obtained from the sequence images previously presented in Fig. 3. The first contour has 64 points and the second one has 58 points. Fig. 9(a) shows the obtained match using the local search adopted in the previous work and Fig. 9(b) shows the one obtained using the proposed global search. Table 1 presents some numerical results for this example. Using the proposed global search 100% of matches of type "one to one" was successfully obtained. Using the local search was only obtained 72% of those matches.

Table 1. Numeric results of the matching between the dynamic pedobarography contours

Search method	Nr. Matches (%)	Fig.
Local	42 (72%)	9 (a)
Global	58 (100%)	9 (b)

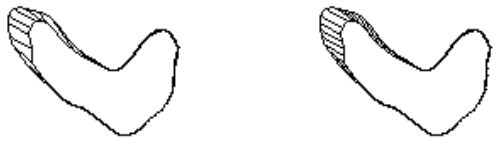

(a) (b)

Fig. 9. Matches between two contours using: (a) the local search; (b) the global search

The second example presents the matching between two isobaric contours, obtained from the previously presented image in Fig. 3(b). The first isobaric contour is composed by 54 points and the second one by 46 points. Fig. 10(a) shows the matching result using the local search and Fig. 10(b) shows the matching result using the proposed global search. Table 2 presents some numerical results for this example. Using the proposed global search we obtained 100% of type "one to one" satisfactory matches. Using the local search we only obtained 50% of those matches.

Table 2. Numeric results of the matching between two isobaric contours

Search method	Nr. Matches (%)	Fig.
Local	23 (50%)	10 (a)
Global	46 (100%)	10 (b)

(a) (b)

Fig. 10. Matches between two isobaric contours using: (a) the local search; (b) the global search

Fig. 11 presents the matching results for the first and second examples using the proposed global matching search and the developed *ADCom* algorithm to match the excess nodes. As it can be seen, all objects' nodes were successfully matched for both examples.

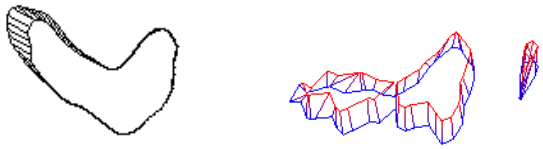

(a) (b)

Fig. 11. (a) Matches between two contours using the global search and *ADCom* algorithm; (b) Matches between two isobaric contours using the global search and *ADCom* algorithm

The last example presents the matching of two surfaces obtained from the same images presented in Fig. 3. The first surface, obtained from the image in Fig. 3(a), has 117 points and the second one, obtained from the image in Fig. 3(b), has 112 points. Fig. 12(a) shows the matching result using the local search and Fig. 12(b) shows the matching result using the proposed global search. Table 3 presents some numerical results of this last example. Using the global search 100% of satisfactory matches of type "one to one" was established. Using the local search was only established 31% of those matches.

6 Conclusions

A methodology was presented for obtaining the correspondence between 2D and 3D objects, rigid or non-rigid, and it was illustrated for real dynamic pedobarography images. The objects are modelled by finite elements and modal analysis is used to define an eigenspace where the matching is performed.

The experimental tests carried out (some shown in this paper) confirm that satisfactory matching results can be obtained for dynamic pedobarographic image data.

Table 3. Numeric results of the matching between two dynamic pedobarography surfaces

Search method	Nr. Matches (%)	Fig.
Local	35 (31%)	12 (a)
Global	112 (100%)	12 (b)

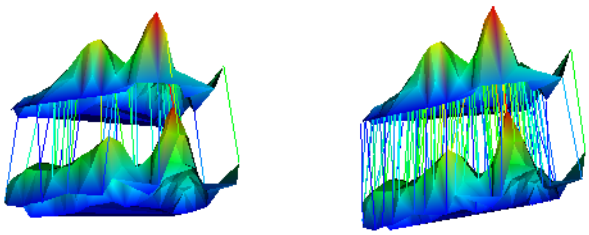

(a) (b)

Fig. 12. Matches between two surfaces using: (a) the local search; (b) the global search

It is also verified that the proposed global search considerably improves these results, when compared with the previously local search used in [2], [13], in the obtained number and in the quality of the founded matches.

Another advantage of the proposed search strategy, based on optimization techniques, is that the overall matching methodology becomes easier to use and to adapt to experimental applications.

The developed *ADCom* algorithm satisfactorily matches all the excess objects nodes, avoiding loss of information along image sequences.

In the future, we will try to improve the matching methodology just presented in order to considerer all the images sequence and use this along time information in the nodes correspondence establishment process.

References

1. S. E. Sclaroff and A. Pentland, "Modal Matching for Correspondence and Recognition", *IEEE Transactions on Pattern Analysis and Machine Intelligence*, vol. 17, 1995
2. J. M. R. S. Tavares, "Análise de Movimento de Corpos Deformáveis usando Visão Computacional", in *Faculdade de Engenharia da Universidade do Porto*, Portugal, 2000
3. Y. Ohta and T. Kanade, "Stereo by Intra- and Inter-Scanline Search using Dynamic Programming," IEEE Transactions on Pattern Analysis and Machine Intelligence, vol. 7, pp. 139-155, 1985
4. S. Roy and I. J. Cox, "A Maximum-Flow Formulation of the N-camera Stereo Correspondence Problem," presented at International Conference on Computer Vision (ICCV'98), Bombay, India, 1998
5. S. Gold, A. Rangarajan, C. P. La, S. Pappu, and E. Mjolsness, "New algorithms for 2D and 3D point matching: pose estimation and correspondence," Pattern Recognition, vol. 31, pp. 1019-1031, 1998

6. C. Silva, "3D Motion and Dense Structure Estimation: Representation for Visual Perception and the Interpretation of Occlusions," in Instituto Superior Técnico: Universidade Técnica de Lisboa, 2001
7. J. L. Maciel and J. P. Costeira, "A Global Solution to Sparse Correspondence Problems," IEEE Transactions on Pattern Analysis and Machine Intelligence, vol. 25, pp. 187-199, 2003
8. Z. Zhang, "Iterative Point Matching for Registration of Free-Form Curves," INRIA, Technical Report RR-1658, April 1992
9. M. S. Wu and J. J. Leou, "A Bipartite Matching Approach to Feature Correspondence in Stereo Vision," Pattern Recognition Letters, vol. 16, pp. 23-31, 1995
10. J. P. P. Starink and E. Backer, "Finding Point Correspondences using Simulated Annealing," Pattern Recognition, vol. 28, pp. 231-240, 1995
11. S. Belongie, J. Malik and J. Puzicha, "Shape Matching and Object Recognition using Shape Context," IEEE Transactions on Pattern Analysis and Machine Intelligence, vol. 24, pp. 509-522, 2002
12. A. J. Padilha, L. A. Serra, S. A. Pires, and A. F. N. Silva, "Caracterização Espacio-Temporal de Pressões Plantares em Pedobarografia Dinâmica", FEUP/INEB 1995
13. J. M. R. S. Tavares, J. Barbosa, and A. Padilha, "Matching Image Objects in Dynamic Pedobarography", presented at *11th Portuguese Conference on Pattern Recognition (RecPad'00)*, Porto, Portugal, 2000
14. T. F. Cootes, C. J. Taylor, “Modelling Object Appearence Using The Grey-Level Surface”, presented at *British Machine Vision Coference*, 1994
15. B. Moghaddam, C. Nastar, A. P. Pentland, “Bayesian Face Recognition using Deformable Intensity Surfaces”, MIT Media Laboratory - Technical Report Nº 371, 1996
16. K.-J. Bathe, *Finite Element Procedures*, Prentice Hall, 1996
17. S. Graham Kelly, *Fundamentals of Mechanical Vibrations*, McGraw-Hill, 1993
18. L. F. Bastos and J. M. R. S. Tavares, "Optimization in Modal Matching for Correspondence of Objects Nodal Points", presented at *7th Portuguese Conference on Biomedical Engineering (BioEng'2003)*, Fundação Calouste Gulbenkian, Lisboa, Portugal, 2003
19. F. S. Hillier and G. J. Lieberman, *Introduction to Operations Research*. Mcgraw-Hill International Editions, 1995
20. L. F. Bastos, "Optimização da Determinação das Correspondências entre Objectos Deformáveis no Espaço Modal", in *Faculdades de Engenharia e Ciências*: Universidade do Porto, Portugal, 2003
21. A. Löbel, "MFC - A Network Simplex Implementation": Konrad-Zuse-Zentrum für Informationstechnik Berlin, Division Scientific Computing, Department Optimization, 2000
22. A. Volgenant, "Linear and Semi-Assignment Problems: A Core Oriented Approach", *Computers and Operations Research*, vol. 23, 1996
23. J. M. R. S. Tavares, J. Barbosa, and A. Padilha, "Apresentação de um Banco de Desenvolvimento e Ensaio para Objectos Deformáveis," *Revista Electrónica de Sistemas de Informação*, vol. 1, 2002
24. R. Davies, *Newmat, A matrix library in C++*, 2003
25. W. Schroeder and K. Martin, *The VTK User’s Guide*, Kitware Inc., 2003
26. W. Schroeder and K. Martin, B. Lorensen, *The Visualization Toolkit*, 3nd Edition, Kitware Inc., 2002